ELSEVIER

Thin Solid Films 374 (2000) 64–69

thin solid films

www.elsevier.com/locate/tsf

Calculations of the atomic structure of the $KNbO_3$ (110) surface

E. Heifets[a], E. Kotomin[b,c,*], P.W.M. Jacobs[d]

[a] *Materials and Processes Simulation Center, Beckman Institute, Caltech, Pasadena, CA 91125, USA*
[b] *Max-Planck Institut für Festkörperforschung, Heisenbergstr., 1, Stuttgart 70569, Germany*
[c] *Institute of Solid State Physics, University of Latvia, 8 Kengaraga, Riga LV-1063, Latvia*
[d] *Department of Chemistry, The University of Western Ontario, London, N6A 5B7, Canada*

Received 25 January 2000; received in revised form 25 April 2000; accepted 24 May 2000

Abstract

The O-terminated $KNbO_3$ (110) surface is modeled using a semi-empirical shell model and two different short-range interatomic potentials. We find this surface to be unstable with respect to a strong reconstruction and K-termination. This conclusion is confirmed by preliminary calculations using the ab initio linear combination of atomic orbitals (LCAO) formalism.

Keywords: Atomistic simulations; Surface and interface states; Perovskites; $KNbO_3$

1. Introduction

Thin ABO_3 ferroelectric films are important for the development of high capacity non-volatile memory components, catalysis, optical waveguides and integrated optics applications. They are also widely used as substrates for growth of the high T_c cuprate superconductors [1,2]. $KNbO_3$, in particular, has highly nonlinear optical coefficients which makes it a promising material for frequency conversion of infrared light into the visible range. This is why in recent years a series of experimental studies have been performed on $KNbO_3$ surfaces, focusing mainly on the (110) surface [3–10]. However, so far there is no information about its atomic structure. In this paper, we calculate for the first time the atomic structure and relaxation of the $KNbO_3$ (110) surface in the cubic (paraelectric) phase.

2. Methods and surface model

In the present study we used a periodic two-dimensional $KNbO_3$ slab. In surface relaxation calculations we optimized the atomic positions in several (1–16) near-surface planes, in the electrostatic field of the slab (simulated by 20 additional planes whose atoms were fixed in their perfect lattice sites). The number of these additional planes was chosen to reach convergence of the crystalline field in the surface planes. Optimisation of so many atomic coordinates cannot be done using ab initio methods, so in this pilot study we used the semi-empirical shell model (SM) [11,12] which has been widely and successfully used earlier for many oxides.

In the SM approach each ion has a charged core and electronic shell. The sum of the core and shell charges is equal to the formal charge on the ion. The use of integer ionic charges does not imply a restriction to ionic materials; in fact the short-range potential effectively takes into account covalency and charge-transfer effects. A harmonic spring constant k connects the core and the shell of the same ion so that the core–shell

* Corresponding author. Fax: +49-711-6891722.
E-mail address: kotomin@chemix.mpi-stuttgart.mpg.de (E. Kotomin).

0040-6090/00/$ - see front matter
PII: S0040-6090(00)01069-5

separation serves as a measure of the atom polarization. The interactions between the cores and between cores and shells of different ions are Coulombic whereas the interactions between the shells of different ions contain, besides the Coulombic part, short-range potentials which account for the effects of exchange repulsion and van der Waals attraction. The short-range Buckingham potentials used here are of the usual form and contain the repulsive parameter A, the hardness parameter ρ, and van der Waals coefficient C for each pair of ions.

The first attempt to develop a SM parameterization for $KNbO_3$ was done by Donnerberg [13]. This model, which neglected the electron shell on K atoms, gave reasonable defect formation energies for bulk $KNbO_3$ but had the disadvantage of producing a negative eigenvalue for the soft (lowest transverse optical, TO) phonon mode. Simultaneously, another set of more refined potentials was developed by Migoni et al. in the framework of their non-linear oxygen polarizability model [14]. These potentials are suited for the correct reproduction of the sequence of energy minima for the Nb off-center displacements along the (100), (110) and (111) axes which correspond to the three ferroelectric transitions which occur when the sample temperature is decreased. In this study we focus on the properties of $KNbO_3$ surface in the high-temperature cubic phase where there is no need for such refined potentials and therefore we employ Buckingham potentials which are used in the standard SM codes.

The above-mentioned disadvantage of the potentials [13] was recently improved [15] by fitting parameters to the relevant frequency at the Γ point of the Brillouin zone (BZ) (at 710 K when $KNbO_3$ has the cubic structure). The two potentials developed — without a shell on the K ion and with such a shell which makes the K ion polarizable — are presented in Tables 1 and 2. They reproduce well six longitudinal optical (LO) and TO frequencies, elastic constants and permittivities. The calculated activation energies for the defect diffusion in the bulk are also in good agreement with quantum chemical calculations and experimental data [15]. In this paper atomistic surface relaxations are calculated by means of the MARVIN computer code [16]. This code permits simulations of complex surface structures using the SM. It was used successfully in our recent calculations of the $SrTiO_3$ (100) [17] and (110) surfaces [18].

Table 1
Two sets of parameters for the shell model for $KNbO_3$ [15], using the Buckingham potentials $A\exp(-r/\rho) - C/r^6$

Interaction	A, eV	ρ, Å	C, eVÅ^6
A. *No shells on K ions*			
O shell–O shell	22746.3	0.1499	27.88
O shell–K core	600.3	0.36198	0.0
O shell–Nb shell	1332.1	0.36404	0.0
B. *With shells on K ions*			
O shell–O shell	22746.3	0.1499	27.88
O shell–K shell	640.0	0.36198	0.0
O shell–Nb shell	1334.8	0.36404	0.0

A problem with the O-terminated (110) surface in $KNbO_3$, which is shown schematically in Fig. 1a,b is that it consists of charged planes. As discussed by Tasker [19], simplest stable crystalline surfaces are electrically neutral with equal numbers of anions and cations on each plane (type-1 surfaces). Crystalline surfaces can also be charged but having no dipole moment perpendicular to the surface due to symmetrical stacking sequence (type-2 surfaces). Lastly, the type-3 surfaces are both charged and have dipole moment in the repeat unit cell perpendicular to the surface. The lattice sums in the electrostatic energy for such surfaces diverge and the calculated surface energy is infinite, which means that surfaces are unstable. If the (110) $KNbO_3$ surface would be modelled directly as it appears after the crystal's cut, it has an infinite dipole moment perpendicular to the surface. To avoid this problem, in our calculations we removed half of O atoms from the O-terminated surface, as we did before for $SrTiO_3$ [18]. Consequently, the surface unit cell is built up of an integer number of neutral fragments which are included in the ellipses shown in Fig. 1c,d. As a result, we obtain the type-II surface having no dipole moment. This is the simplest atomistic model for this kind of at surfaces. In the future we plan to study more complicated models with steps and reconstruction.

We start calculations with the reference geometry A (Fig. 1c) and then study its relaxation for the two types of interatomic potentials (which results in two final geometries A1 and A2, respectively). When doing so, all atoms in 16 near-surface planes are allowed to move along the y and z axes parallel and perpendicular to the surface, respectively, during minimization of the total energy (Fig. 1e,f). Since simple removal of half of O atoms from the surface upsets the balance of intera-

Table 2
Core and shell charges and core–shell spring constants k [15] used in $KNbO_3$ calculation with an electron shell on the K^+ ion

Ion type	Effective charge, e core	Shell	k, eVÅ^{-2}
O	0.811	−2.811	103.07
K	3.76	−2.76	100.00
Nb	9.496	−4.496	2100.0

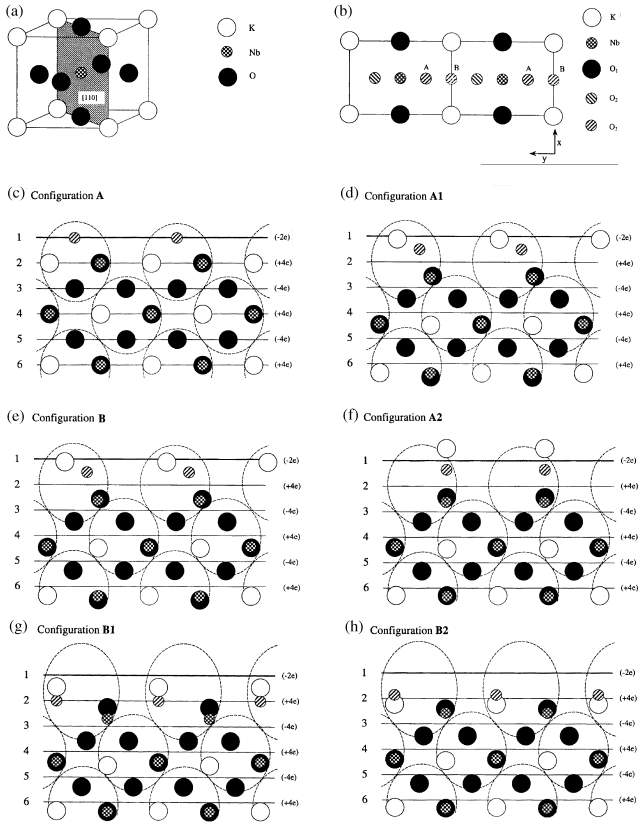

Fig. 1. (a) Sketch of the $KNbO_3$ cubic structure with a shaded O-terminated (110) surface. (b) The top-view, direction of the O displacements along the surface are shown by arrows. In our model we remove oxygen atoms O_2 from the surface, and study atomic relaxations when O_3 atoms are placed initially in the positions either A or B, respectively. Atoms Nb, K and O_1 lie in the second plane below the surface. (c,d) The side-views of the first six planes for O-terminated surface with the starting atomic configurations A and B shown in (b). Dashed ellipses containing five atoms from the three nearest planes show neutral fragments from which the surface unit cell is built whereas numbers in brackets on the right hand side of planes give the corresponding effective charges. (e–h) The relevant final atomic geometries.

tomic interactions, we studied another initial O termination geometry B (Fig. 1b,d), where O atoms are placed more symmetrically, at positions at the mid-point of the distance between the two bulk crystalline O sites, in the vertical plane with K atoms. Therefore, we studied the effect for the O-terminated surface relaxation for the two initial geometries A and B, and for two potential sets (without and with an electron shell on K atoms). As a result, we obtained four relaxation patterns called A1, A2 and B1 and B2, respectively.

To check our semi-empirical findings, ab initio Hartree–Fock calculations based on the linear combination of atomic orbitals (LCAO) basis set were performed for four above mentioned SM geometries. In these calculations we used an isolated two-dimension slab containing 15 planes and 35 atoms per surface cell. The basis set was taken from [20], Hay–Wadt small core pseudopotentials were used for K and Nb atoms. For this purpose, the Crystal-98 computer code was used [21] with the Perdew–Wang–GGA electron correlation corrections to the total energy were included a posteriori [22].

3. Results and discussion

Table 3 and Fig. 1e–h summarize the atomic relaxations found for the two different O termination geometries A and B. In the 'symmetric' B1 case terminating O atoms move strongly inwards, and so do Nb atoms in the second plane. In contrast, K atoms in the second plane move up strongly, in the direction outwards from the surface. Atoms in a whole region containing about 10 near-surface planes are strongly displaced from their lattice sites, as shown by the results for the outermost six planes which are presented in Table 3. This is in strong contrast to the $SrTiO_3$ (100) surface [17]. (Displacements along the $KNbO_3$ surface are very small and are not presented.) When we incorporate electronic shells on the K atoms, the largest change in the final geometry B2 is observed for the K atoms, which now move inwards. Simultaneously, K atoms are strongly polarized, the relative core–shell displacement being 2.6%. This results from the strong Coulomb repulsion of the K electronic shell by O atoms in the first plane and a strong attraction to them of K cores. If we compare these results with previous $SrTiO_3$ (110) calculations containing the shells on Sr atoms, O and Ti atoms were also displaced inwards, but by only 3–5% whereas Sr moved strongly (30%) outwards to the surface. These differences in the two materials are due to the fact that the Sr effective charge is twice as large as that of K.

For the other 'asymmetrical' initial geometry A of a surface with O termination (Fig. 1b,c) when electronic shells are included on K atoms, we found that O atoms move along the y axis on the surface and stop exactly above the Nb atoms in the second plane (A2 pattern shown in Fig. 1f). Then both O and Nb move inwards, by 11% and 19%, respectively. Simultaneously, K atoms in the second plane are shifted in the same y direction, as the terminating O atoms, and also move strongly outwards from the surface along the z axis, so that they end up above the O atoms in the second plane, which are in their turn also displaced outwards from the surface. As a result, the Nb–O distance is reduced by $\approx 8\%$ as compared to that in the bulk. The K atoms in the A2 configuration are even more strongly polarized than in the B2 case (the relative core–shell separation being 3.3%). As a result, K atoms lie above the first plane of the unrelaxed surface and thus in fact terminate the surface. When K atoms have no shells (A1 mode), their outward relaxation is smaller (31%) (Fig.

Table 3
Atomic displacements (in per cent of the bulk lattice constant) for atoms in six near-surface planes on the $KNbO_3$ O-terminated (110) surface (see Fig. 1)[a]

Layer No	Ion	Type	Δz B1 (B2)	Δy A1 (A2)	Δz A1 (A2)
1	O^2	Core	−35.0 (−29.6)	18.6 (35.1)	−16.3 (−10.9)
		Shell	−34.7 (−30.0)	19.4 (35.1)	−18.9 (−13.5)
2	Nb^{+5}	Core	−24.6 (−20.5)	−1.1 (−0.3)	−21.6 (−19.4)
		Shell	−23.6 (−19.5)	−0.8 (−0.3)	−21.8 (−19.6)
	K^{+1}	Core	19.2 (−6.7)	23.5 (70.5)	31.5 (50.2)
		Shell	(−9.3)	(70.5)	(53.5)
	O^{-2}	Core	−13.7 (−13.6)	2.4 (−0.3)	−19.3 (−15.1)
		Shell	−14.2 (−13.9)	2.2 (−0.3)	−19.5 (−15.4)
3	O^{-2}	Core	−20.5 (−17.0)	2.1 (1.0)	−15.3 (−13.6)
		Shell	−19.2 (−15.9)	1.9 (0.6)	−15.6 (−13.6)
4	K^{+1}	Core	−18.9 (−15.7)	0.0 (−0.3)	−17.2 (−16.1)
		Shell	(−15.6)	(−0.3)	(−15.3)
	Nb^{+5}	Core	−14.1 (−12.6)	−0.5 (−0.2)	−14.3 (−11.8)
		Shell	−12.9 (−12.4)	−0.5 (−0.3)	−14.3 (−11.9)
	O^{-2}	Core	−14.7 (−13.6)	−0.5 (−1.5)	−15.9 (−14.2)
		Shell	−14.7 (−13.6)	0.0 (−1.1)	−15.7 (−14.2)
5	O^{-2}	Core	−13.9 (−11.1)	−0.9 (−1.1)	−13.6 (−11.4)
		Shell	−13.9 (−11.9)	−0.7 (−1.2)	−13.7 (−11.6)
6	Nb^{+5}	Core	−13.0 (−11.3)	−0.4 (−0.2)	−12.8 (−11.1)
		Shell	−12.9 (−11.2)	−0.4 (−0.3)	−12.8 (−11.1)
	K^{+1}	Core	−12.1 (−10.3)	−0.3 (−0.3)	−12.3 (−10.1)
		Shell	(−10.5)	(−0.3)	(−10.3)
	O^{-2}	Core	−13.0 (−11.1)	−0.2 (−0.3)	−13.0 (−10.6)
		Shell	−13.0 (−11.1)	−0.2 (−0.3)	−13.0 (−10.6)

[a] Positive and negative signs for Δz mean directions outwards from the surface and inwards the surface, respectively. In total, 16 near-surface planes were allowed to relax. A and B denote the two starting geometries for O atoms in the O-terminated surface (Fig. 1c,d) whereas 1 and 2 refer to cases when K has not and has an electron shell (see Tables 1 and 2).

1e). In similar $SrTiO_3$ calculations we found [18] that O atoms go above Ti atoms, and both shift inwards (by 14% and 2%, respectively) whereas Sr moves slightly up by 4%.

The lattice relaxation energies found for the four geometries studied are given in Table 4. The largest surface relaxation of 7.46 eV occurs for the A2 mode when O atoms initially occupy every second bulk lattice site and K^+ ions are polarizable. The HF-LCAO ab initio calculations (Table 4) also show that the lowest total energy corresponds to A2 geometry, which confirms our SM findings. We have checked that this ab initio result does not depend on a particular choice of the electron correlation functional available in the Crystal code; the relevant variation in total energies is considerably smaller than the relaxation energies under study.

The effective (static) atomic charges calculated using the Mulliken analysis show that those for Nb and O in the middle plane modeling the bulk are $+3.0\ e$ and $-1.33\ e$, respectively, is in contrast to the ionic model ($+5.0\ e$ and $-2.0\ e$). This means considerable covalency between Nb and O whereas K is almost completely ionized ($+0.97\ e$). In the optimised A2 configuration there is an additional 0.06 e transferred from surface O atoms to the Nb atoms below them.

The difference in surface geometries from our previous $SrTiO_3$ calculations [18] comes from the fact that K atoms are smaller in size and have half the effective charge of Sr atoms, which makes their displacement easier. Starting with the two different initial termination geometries A and B, we obtained two quite different relaxation patterns. Probably, this arises from the complex energy surface of the system with an energy barrier between these two configurations.

In Fig. 2 the values of surface dipole moments perpendicular to the surface are plotted for the four cases discussed above, as a function of the number of relaxed layers. Similarly to our earlier observation for the $SrTiO_3$ (100) surface, the dipole moments strongly oscillate before reaching saturation as the number of re-

Table 4
The ab initio LCAO total energies for slabs of four different geometries found in the shell model calculations and the slab relaxation energies as found in the shell model (in eV per the surface unit cell). The total energies are given with the reference to the largest, B1 energy

Energy	B1	B2	A1	A2
ΔE_{tot}	0.0	−13.85	−3.34	−15.78
E_{rel}	−5.76	−4.83	−6.83	−7.46

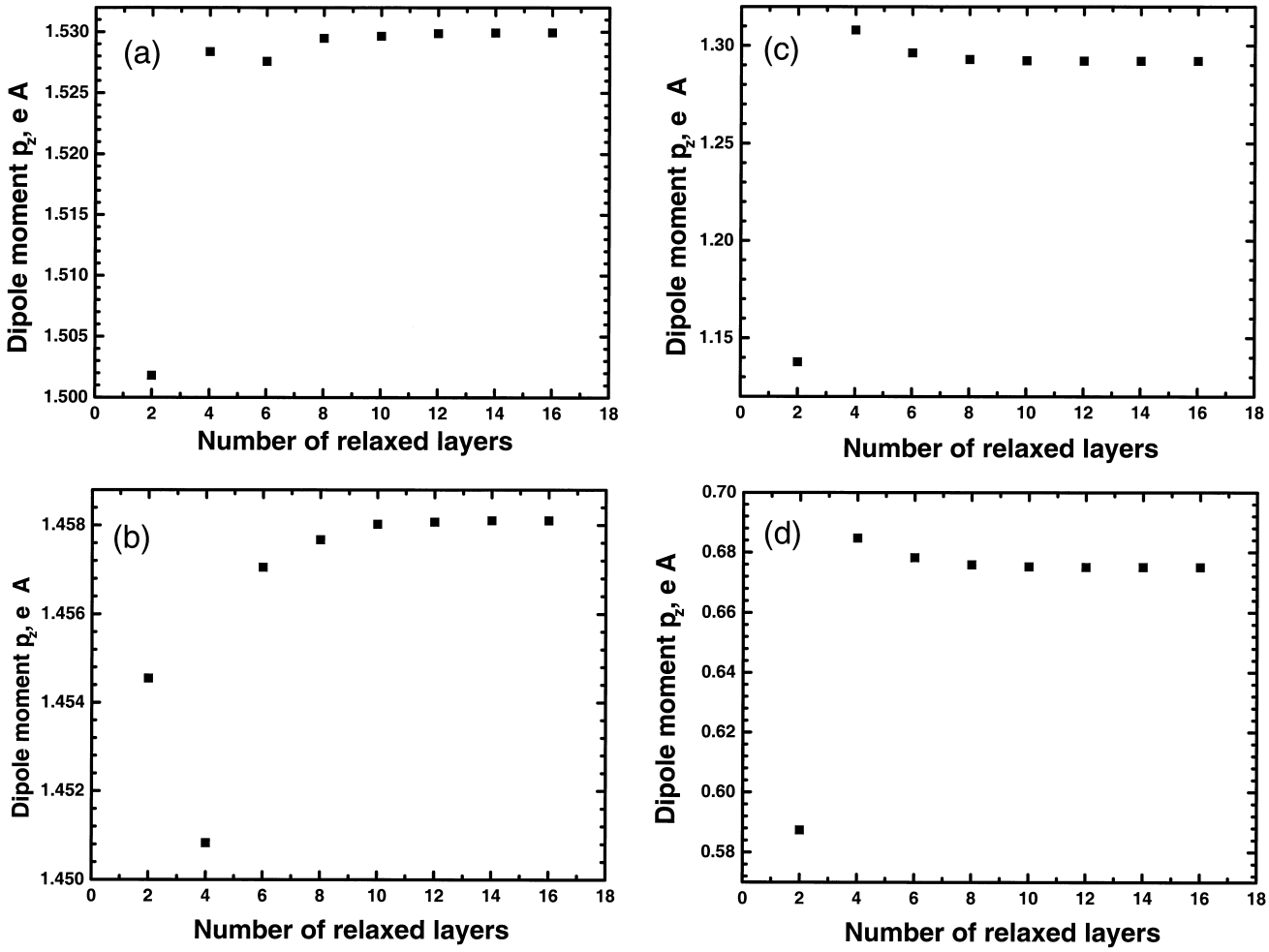

Fig. 2. Surface-induced dipole moments perpendicular to the surface as a function of number of near-surface layers allowed to relax on the O-terminated $KNbO_3$ calculated for the A1, A2, B1 and B2 geometries, shown in (a–d), respectively.

laxed planes reaches approximately 10. This is a critical bottleneck for ab initio calculations where typically one–two planes are relaxed only. Due to huge atomic relaxations the calculated values of dipole moments are about an order of magnitude larger than those found for the (100) surface [17]. There is also a big difference in the saturated values for A1 and A2 geometries, which stresses once more the importance of the proper treatment of K polarizability.

In summary, our calculations have shown that the stoichiometric O-terminated (110) surface in $KNbO_3$ — unlike $SrTiO_3$ [18] — is unstable with respect to strong relaxation, and even K-termination. This is in line with an experimental study [23] which demonstrated that the $KNbO_3$ surface region has a quite complicated chemical composition very different from the bulk material, which gives rise to an observed anomalous hysteresis loops. Large surface-induced dipole moments indicate that ferroelectric properties of thin (110) films could be quite different from those of the bulk perovskite crystal. Another, methodological conclusion is that incorporation of K ion polarizability is very important inperovskite surface modeling. Study of other $KNbO_3$ surface terminations are in progress.

Acknowledgements

The authors are indebted to D. Fuks, S. Dorfman, C.R.A. Catlow, R. De Souza, and J. Maier for fruitful discussions.

References

[1] V.E. Henrick, P.A. Cox, The Surface Science of Metal Oxides, Cambridge University Press, NY, 1994.
[2] M.E. Lines, A.M. Glass, Principles and Applications of Ferroelectrics and Related Materials, Clarendon, Oxford, 1977.
[3] T. Graettinger, P.A. Morris, A. Roshko, A.I. Kingon, O. Auciello, D.J. Lichtenwalner, A.F. Chow, Mater. Res. Soc. Symp. Proc. 341 (1994) 265.
[4] T. Graettinger, D.J. Lichtenwalner, A.F. Chow, O. Auciello, A.I. Kingon, Integrated Ferroelectrics 6 (1995) 363.

[5] M.J. Martin, J.E. Alfonso, J. Mendiola, C. Zaldo, D.S. Gill, R.W. Eason, P.J. Chandler, J Mater. Res. 12 (1997) 2699.
[6] C. Zaldo, D.S. Gill, R.W. Eason, J. Mendiola, P.J. Chandler, Appl. Phys. Lett. 65 (1994) 502.
[7] H.-M. Christen, L.A. Boatner, J.D. Budai, M.F. Chisholm, L.A. Gea, P.J. Marrero, D.A. Norton, Appl. Phys. Lett. 68 (1996) 1488.
[8] A. Onoe, A. Yoshida, K. Chikuma, Appl. Phys. Lett. 69 (1996) 167.
[9] R.F. Xiao, H.D. Sun, Y.Y. Siu, Y.Y. Zhu, P. Yu, G.K.L. Wong, Appl. Phys. Lett. 70 (1997) 164.
[10] E.D. Specht, H.-M. Christen, D.P. Norton, L.A. Boatner, Phys. Rev. Lett. 80 (1998) 4317.
[11] C.R.A. Catlow and W.C. Mackrodt (Eds.) Computer Simulations of Solids, *Lecture Notes in Physics*, Vol. 166, Springer Verlag, Berlin, 1982.
[12] H.J. Donnerberg, BerlinAtomic Simulations of Electrooptic and Magnetooptic Oxide Materials Springer Tracts in Modern Physics Volume 151, 1999.
[13] H.J. Donnerberg, M. Exner, Phys. Rev. B49 (1994) 3746.
[14] M. Sepliarsky, M.G. Stachiotti, R.L. Migoni, Phys. Rev. B52 4044; ibid. B56 (1997) (1995) 566.
[15] P.W.M. Jacobs, E.A. Kotomin, R. Eglitis, J. Phys.: Condens. Matter 12 (2000) 569.
[16] D.H. Gay, A.L. Rohl, J. Chem. Soc. Faraday Trans. 91 (1995) 925.
[17] E. Heifets, D. Fuks, S. Dorfman, E.A. Kotomin, J. Phys.: Condens. Matter 10 (1998) L347.
[18] E. Heifets, E.A. Kotomin, Thin Solid Films 358 (2000) 1.
[19] P.W. Tasker, J. Phys. C: Solid State Phys. 12 (1979) 4977.
[20] S. Dalli Olio, R. Dovesi, R. Resta, Phys. Rev. B56 (1997) 10105.
[21] V.R. Saunders, R. Dovesi, C. Roetti, M. Causa, N.M. Harrison, R. Orlando, CM. Zicovich-Wilson, Crystal-98 User Manual, University of Torino, 1999.
[22] J.P. Perdew, Y. Wang, vPhys. Rev. B45 (1992) 13244.
[23] W. Szot, K. Speier, J. Herion, Ch. Freiburg, R. Waser, M. Pawelczyk, W. Eberhardt, J. Phys. Chem. Sol. 57 (1996) 1765.